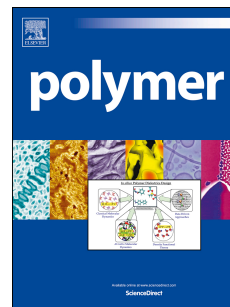


Accepted Manuscript

Tuning the Self-Healing Behavior of One-Component Intrinsic Polymers

J. Kötteritzsch, Dr. M.D. Hager, Prof. Dr. U.S. Schubert



PII: S0032-3861(15)00255-4

DOI: [10.1016/j.polymer.2015.03.027](https://doi.org/10.1016/j.polymer.2015.03.027)

Reference: JPOL 17699

To appear in: *Polymer*

Received Date: 9 December 2014

Revised Date: 9 March 2015

Accepted Date: 10 March 2015

Please cite this article as: Kötteritzsch J, Hager MD, Schubert US, Tuning the Self-Healing Behavior of One-Component Intrinsic Polymers, *Polymer* (2015), doi: 10.1016/j.polymer.2015.03.027.

This is a PDF file of an unedited manuscript that has been accepted for publication. As a service to our customers we are providing this early version of the manuscript. The manuscript will undergo copyediting, typesetting, and review of the resulting proof before it is published in its final form. Please note that during the production process errors may be discovered which could affect the content, and all legal disclaimers that apply to the journal pertain.

Tuning the Self-Healing Behavior of One-Component Intrinsic Polymers

Julia Kötteritzsch, Martin D. Hager* and Ulrich S. Schubert*

J. Kötteritzsch, Dr. M. D. Hager, Prof. Dr. U. S. Schubert

Laboratory for Organic and Macromolecular Chemistry (IOMC), Friedrich Schiller University Jena, Humboldtstr. 10, 07743 Jena, Germany

E-mail: ulrich.schubert@uni-jena.de; martin.hager@uni-jena.de

Phone: +49 3641 9-48220

Fax: +49 3641 9-48202

J. Kötteritzsch, Dr. M. D. Hager, Prof. Dr. U. S. Schubert

Jena Center for Soft Matter (JCSM), Friedrich Schiller University Jena, Philosophenweg 7, 07743 Jena, Germany

Tuning the Self-Healing Behavior of One-Component Intrinsic Polymers

Julia Kötteritzsch, Martin D. Hager* and Ulrich S. Schubert*

Novel terpolymers with furan and maleimide units as functional moieties for the reversible crosslinking by the Diels-Alder (DA) reaction with different polar and nonpolar co-monomers and linkers have been prepared for potential applications as self-healing coatings. The synthesized linear one-component systems are able to crosslink *via* the functional units in the side chain (*i.e.* furan and maleimide) resulting in a highly crosslinked network. The terpolymers contain different maleimide methacrylates with three different linkers (MIMA 1, MIMA 2, MIMA 3), which vary in the length and the composition of the spacer unit as well as furfuryl methacrylate (FMA) as active units. Moreover, as polar co-monomers hydroxyethyl methacrylate (HEMA), dimethylaminoethyl methacrylate (DMAEMA) as well as 2-(hydroxyethoxy)ethyl methacrylate (DEGMA) and as nonpolar co-monomer butyl methacrylate (BMA) were used. The terpolymers were characterized using ^1H NMR spectroscopy and SEC measurements; the thermal properties were studied by TGA and DSC investigations as well as the self-healing properties by real-time analyses using a microscope equipped with a camera.

Keywords: copolymerization; crosslinking; Diels-Alder cycloaddition; self-healing polymers; microscope images; polar co-monomers

1. Introduction

Self-healing materials are in focus of interest in recent years. In particular, the Diels-Alder (DA) cycloaddition has been applied in many materials to achieve intrinsic self-healing abilities without changing significantly the original properties of the materials [1–3]. By this manner, it is possible to access self-healing polymers with well-defined architectures and properties, due to the thermal reversibility (retro-Diels-Alder reaction) [4,5]. The Diels-Alder chemistry was widely utilized in polymer as well as material science [1,6–10]. Later, Wudl and coworkers introduced this concept into the field of self-healing (remendable) polymers [2,11–13].

The first synthesis of a functional copolymer based on methacrylates was reported by Wouters and Fischer *et al.* in 2009 and additionally by Haddleton and coworkers in 2010 [14,15]. The first investigations on the synthesis of PFMA *via* ATRP and free radical polymerization (FRP) and the copolymerization with methyl methacrylate (MMA) were published by Kavitha and Singha as well as the synthesis of a PFMA-*b*-PEHA-*b*-PFMA triblock copolymer. The authors also studied the self-healing properties of the copolymer [16–19].

Our previous work was based on these investigations and we could create a one-component intrinsic self-healing coating based on the reversible DA reaction. For this purpose we incorporated both functionalities for the DA reaction, *i.e.*, furan as well as maleimide units, into linear polymers based on a methacrylate backbone [20]. As a consequence no additional (low molar mass) crosslinkers are required to crosslink the polymer and to achieve the desired self-healing properties. The self-healing properties of the most promising terpolymer P(LMA-*co*-MIMA-*co*-FMA) were further investigated by Bose *et al.* [21]. Barthel *et al.* extended the concept to functional block copolymers [22–24].

One drawback of the Diels-Alder cycloaddition of maleimide and furan is the required high temperature (120 to 180 °C) of the rDA [20]. In our previous work the DSC measurements and the self-healing studies of the copolymers P(AMA-*co*-FMA-*co*-MIMA) revealed that the variation of the chain length of the co-monomers influenced the temperature of the retro-Diels-Alder reaction: More nonpolar environments resulted in higher temperatures of the retro-Diels-Alder reaction [20]. This effect was also observed by Kavitha and Singha [16–19]. Additionally, other studies revealed that more polar environments of the maleimide/furan unit resulted in a slightly decreased rDA temperature [25–28]. Toncelli *et al.* pointed out that at relatively low maleimide/furan ratio the RDA transitions become broader and shift asymmetrically towards lower temperatures, while the crosslinking density drops significantly. This is due to the decrease of the furan content and, therefore, an increase of the mobility of the chains appears [28]. Similar effects of the polarity on the activation energy (E_A) of the rDA of small molecules were reported by Wijnen *et al.* [29], Rispens *et al.* [30] and Kiseleva *et al.* [31]. The authors indicated that polar solvents have a significant influence on the equilibrium of the Diels-Alder reaction and on the activation energy of the retro-Diels-Alder reaction. As a consequence we decided to investigate if the incorporation of a polar co-monomer (HEMA, DMAEMA and DEGMA) into the terpolymer with Diels-Alder functionalities could also decrease the rDA temperature. Furthermore, this factor could also be useful to improve the self-healing behavior of the copolymers.

A restriction in this case is the relatively high glass transition temperature of these monomers compared to lauryl methacrylate (LMA), which revealed up to now the best self-healing properties [20]. As reported by Mayo and Adronov also the linker unit has a significant influence on the hardness of the film as well as the film-forming behavior of the system [32]. An enhanced mobility of the system promotes the self-healing

properties at lower temperatures due to the required backflow of the material into the scratch after reaching the rDA temperature.

Therefore, also different linkers of the maleimide methacrylate monomers were used to improve the flexibility and mobility of the copolymers, because this represents an important prerequisite for the potential self-healing abilities of our one-component self-healing system at lower temperatures.

2. Experimental Procedures

2.1 Materials and Instrumentation

All chemicals were purchased from Fluka, Aldrich, Acros Organics as well as Alfa Aesar and were used without further purification unless otherwise specified. The solvents were purchased from Biosolve, Aldrich as well as Acros Organics. Dry dichloromethane and toluene were obtained from a PureSolv-EN Solvent Purification System (Innovative Technology). Triethylamine was dried over calcium chloride.

1D (^1H , ^{13}C) nuclear magnetic resonance spectra were recorded on a Bruker AC 400 (400 MHz), Bruker AC 300 (300 MHz) and Bruker AC 250 (250 MHz) at 298 K. Chemical shifts are reported in parts per million (ppm, δ scale) relative to the residual signal of the solvent. Coupling constants are given in Hz.

CHN analysis was carried out on a Vario El III (Elementar) elemental analyzer.

ESI-TOF MS measurements were performed using a micrOTOF (Bruker Daltonics) mass spectrometer, which was equipped with a syringe pump for sample injection and a standard electrospray ion source. The mass spectrometer was operating in the positive ion mode and the data were processed with the micrOTOF control Version 3.0 and Data

Analysis Version 4.0 SP2. The instrument was calibrated by a tunemix solution (m/z 50 to 3,000) from Agilent.

Size exclusion chromatography measurements were performed on an Agilent 1200 system (degasser, isocratic pump, autosampler, RI detector) and two PSS GRAM (1000/30 Å, 10 µm particle size) columns in series (eluent: DMAc with 2.1 g/L LiCl; flow rate of 1 mL/min at 40 °C) using linear poly(methyl methacrylate) standards.

The TGA analysis (TGA) was carried out using a Netzsch TG 209 F1 and the differential scanning calorimetry (DSC) measurements were performed on a DSC 204 F1 Phoenix by Netzsch under a nitrogen atmosphere with a heating rate of 20 K min⁻¹.

The simultaneous thermal analysis (STA) was carried out using the Netzsch 449 F3 Jupiter with a Netzsch QMS 403 D Aëolos MS detector and a Bruker Tensor 27 FT-IR detector.

Optical micrographs of the sample were acquired with the optical detection unit of the AFM facility. For this purpose, the films were crosslinked for 4 h between 120 to 130 °C, scratched with a hollow needle or a knife in a controlled manner and annealed for individual timescales to obtain the different healing states at different temperatures.

2.2 Synthesis

The monomers MIMA 1 to MIMA 3 and the corresponding precursors were synthesized according to Kötteritzsch *et al.* [20]. The synthesis of the copolymers **P1** to **P7** was also performed using similar conditions as described by Kötteritzsch *et al.* [20]. Only the reaction conditions for the terpolymers with the polar co-monomers (**P1**, **P2** and **P4**) were varied due to the better solubility of the monomers and the resulting polymers in polar solvents [33,34].

Synthesis of 2-(6-hydroxyhexyl)-3a,4,7,7a-tetrahydro-1H-4,7-epoxyisoindole-1,3(2H)-dione (3)

3a,4,7,7a-Tetrahydro-4,7-epoxyisobenzofuran-1,3-dione (2.0 g, 12.1 mmol) and methanol (50 mL) were added into a three-neck round-bottom flask containing a magnetic stirring bar and a reflux condenser. The solution was purged with nitrogen for 10 min in an ice bath. Subsequently, 6-aminohexan-1-ol (1.4 g, 12.1 mmol) and triethylamine (1.7 mL, 12.1 mmol) were added. The reaction mixture was allowed to warm to room temperature and the temperature was later increased to 67 °C for 20 h. Subsequently, 10% of 6-aminohexan-1-ol (0.14 g, 1.2 mmol) was added and stirring was continued for 2 h at 70 °C. The solution turned dark orange. The flask was cooled to room temperature and the solution volume was reduced to dryness. Subsequently, the orange oil was dissolved in dichloromethane, washed with water and dried over MgSO₄. The product was precipitated in ice-cold hexane and stored at -22 °C. The precipitate was collected *by* decantation and used without further purification. Yield 1.1 g (35%).
¹H NMR (250 MHz, CDCl₃): δ = 6.50 (s, 2H, CH), 5.25 (s, 2H, CH), 3.60 (t, *J* = 6.3 Hz, 2H, CH₂), 3.47 (t, *J* = 7.2 Hz, 2H, CH₂), 2.82 (s, 2H, CH), 1.7 – 1.2 (m, 8H, CH₂).
¹³C NMR (62.9 MHz, CDCl₃): δ = 176.3 (CO-N), 136.5 (=CH-), 80.9 (>CH-), 62.6 (-CH₂-), 47.4 (>CH-), 38.8 (-CH₂-), 32.4 (-CH₂-), 27.4 (-CH₂-), 26.1 (-CH₂-), 25.0 (-CH₂-). (C₁₄H₁₉NO₄)_n (265.1)_n: Calcd. C 63.38, H 7.22, N 5.28; Found C 63.62, H 7.01, N 4.89.

Synthesis of 2-(2-(2-hydroxyethoxy)ethyl)-3a,4,7,7a-tetrahydro-1H-4,7-epoxyisoindole-1,3(2H)-dione (4)

3a,4,7,7a-Tetrahydro-4,7-epoxyisobenzofuran-1,3-dione (1 g, 6 mmol), methanol (50 mL) and 2-(2-aminoethoxy)ethan-1-ol (0.7 g, 6.7 mmol) were added into a three-

neck round-bottom flask containing a magnetic stirring bar and a reflux condenser. The solution was purged with nitrogen for 10 min in an ice bath. Subsequently, triethylamine (1 mL, 7.2 mmol) was added. The reaction mixture was allowed to warm to room temperature and the temperature was later increased to 67 °C for 20 h. Subsequently, 10% of 2-(2-aminoethoxy)ethan-1-ol (0.07 g, 0.7 mmol) was added and stirring was continued for 2 h at 70 °C. The solution turned dark orange. The flask was cooled to room temperature and the solution volume was reduced to dryness. Subsequently, the orange oil was dissolved in dichloromethane, washed with water and dried over MgSO₄. The product was precipitated in ice-cold hexane and stored at -22 °C. The precipitate was collected *by* decantation and used without further purification. Yield 0.59 g (38%). ¹H NMR (300 MHz, CDCl₃): δ = 6.50 (s, 2H, CH), 5.28 (s, 2H, CH), 3.80 – 3.4 (m, 8H, CH₂), 2.86 (s, 2H, CH), 2.70 (s, 1H, OH). ¹³C NMR (62.9 MHz, CDCl₃): δ = 176.3 (CO-N), 136.4 (=CH-), 81.0 (>CH-), 72.3 (-CH₂-), 67.0 (-CH₂-), 61.6 (-CH₂-), 47.4 (>CH-), 38.5 (-CH₂-). (C₁₂H₁₅NO₅)_n (253.3)_n: Calcd. C 56.91, H 5.97, N 5.53; Found C 56.83, H 6.31, N 5.52.

Synthesis of 6-(1,3-dioxo-1,3,3a,4,7,7a-hexahydro-2H-4,7-epoxyisoindol-2-yl)hexyl methacrylate (MIMA 2)

2-(6-Hydroxyhexyl)-3a,4,7,7a-tetrahydro-1H-4,7-epoxyisoindole-1,3(2H)-dione (0.925 g, 3.6 mmol) was added to a two-neck round bottom flask containing a magnetic stirring bar. After purging the flask with nitrogen, dry dichloromethane (20 mL) and triethylamine (0.8 mL, 5.7 mmol) were added and the reaction solution was cooled to 0 °C with an ice bath. To this solution methacryloyl chloride (0.4 mL, 4.1 mmol) was added dropwise. The reaction was stirred overnight, slowly warming to room temperature. Subsequently, the reaction mixture was quenched with methanol and

afterwards extracted with aqueous NH_4Cl , H_2O and brine. The organic layer was dried over MgSO_4 , filtered and reduced in vacuum. The product was further purified *via* column chromatography (silica, ethyl acetate as eluent). Yield 0.667 g (55%). ^1H NMR (300 MHz, CDCl_3): δ = 6.51 (s, 2H, **CH**), 6.09 (s, 1H, **CH**), 5.55 (s, 1H, **CH**), 5.26 (s, 2H, **CH**), 4.11 (t, J = 6.6 Hz, 2H, **CH₂**), 3.46 (t, J = 7.3 Hz, 2H, **CH₂**), 2.84 (s, 2H, **CH**), 1.93 (s, 3H, **CH₃**), 1.8 – 1.5 (m, 4H, **CH₂**), 1.5 – 1.2 (m, 4H, **CH₂**). ^{13}C NMR (62.9 MHz, CDCl_3): δ = 176.3 (-CO-N), 167.5 (>CO), 136.5 (=CH-), 136.5 (>C=), 125.2 (>C=), 80.9 (>CH-), 64.5 (-CH₂-), 47.4 (>CH-), 38.8 (-CH₂-), 28.4 (-CH₂-), 27.4 (-CH₂-), 26.2 (-CH₂-), 25.5 (-CH₂-), 18.3 (-CH₃). $(\text{C}_{18}\text{H}_{23}\text{NO}_5)_n$ (333.2)_n: Calcd. C 64.85, H 6.95, N 4.20; Found C 64.77, H 7.08, N 3.97.

Synthesis of 2-(2-(1,3-dioxo-1,3,3a,4,7,7a-hexahydro-2H-4,7-epoxyisoindol-2-yl)ethoxy)ethyl methacrylate (MIMA 3)

2-(2-(2-Hydroxyethoxy)ethyl)-3a,4,7,7a-tetrahydro-1H-4,7-epoxyisoindole-1,3(2H)-dione (0.5 g, 2 mmol) was added into a two-neck round bottom flask containing a magnetic stirring bar. After purging the flask with nitrogen, dry dichloromethane (10 mL) and triethylamine (0.4 mL, 2.9 mmol) were added and the reaction solution was cooled to 0 °C with an ice bath. To this solution methacryloyl chloride (0.3 mL, 3.1 mmol) was added dropwise. The reaction was stirred overnight, slowly warming to room temperature. Subsequently, the reaction mixture was quenched with methanol and afterwards extracted with aqueous NH_4Cl , H_2O and brine. The organic layer was dried over MgSO_4 , filtered and reduced in vacuum. The product was further purified *via* column chromatography (silica, ethyl acetate as eluent). Yield 0.5 g (79%). ^1H NMR (300 MHz, CDCl_3): δ = 6.52 (s, 2H, **CH**), 6.13 (s, 1H, **CH**), 5.58 (s, 1H, **CH**), 5.27 (s, 2H, **CH**), 4.25 (t, J = 4.8 Hz, 2H, **CH₂**), 3.8 -3.6 (m, 6H, **CH₂**), 2.87 (s, 2H, **CH**), 1.95

(s, 3H, CH₃). ¹³C NMR (62.9 MHz, CDCl₃): δ = 176.1 (-CO-N), 167.3 (>CO), 136.5 (=CH-), 136.1 (>C=), 125.7 (>C=), 80.9 (>CH-), 68.6 (-CH₂-), 67.1 (-CH₂-), 63.8 (-CH₂-), 47.4 (>CH-), 38.1 (-CH₂-), 18.3 (-CH₃). HR-ESI-TOF MS: [C₁₆H₁₉NO₆]^{Na+} calcd.: m/z = 344.1105; found: m/z = 344.1102; error: 0.8 ppm.

General procedure for the synthesis of copolymers P(RMA-co-FMA-co-MIMA) (P1 to P7)

CuBr (2 eq.), HMTETA (2 eq.), RMA, FMA, the maleimide monomer (MIMA 1, MIMA 2 or MIMA 3) and toluene or DMF (for **P1**, **P2** and **P4**) (2 mL) were added to a vial containing a stirring bar. The polymerization was initiated by adding EB*i*B (1 eq. or 2 eq.) and was carried out at 70 °C or room temperature (for **P1**, **P2** and **P4**) under a nitrogen atmosphere. The reaction was stopped after 2 to 4 h. The polymer was purified by passing the solution through an alumina column to remove the catalyst, precipitation in ice-cold diethylether or *n*-hexane and drying in an IR Dancer (Hettlab) at room temperature. Also later purification by preparative size exclusion chromatography using a Biobeads[®] S-X1 column was performed for **P4** to **P7**. Parts of the polymer samples were analyzed by size exclusion chromatography (SEC) to determine the molar mass and molar mass distribution.

3. Results and Discussion

3.1 Synthesis of the Maleimide Methacrylates (MIMA 1 to MIMA 3)

The synthesis of the new maleimide methacrylate monomers (MIMA 1, MIMA 2 and MIMA 3) is depicted in **Scheme 1**. The first step is a Diels-Alder reaction between furan and maleimide as described by Kötteritzsch *et al.* [20]. Subsequently, compound **1** was reacted *via* an amine insertion with different amino alcohols. The last reaction step

was the esterification of the compounds **2** to **4** with methacryloyl chloride to yield MIMA 1, MIMA 2 and MIMA 3. The characterization of the monomers was performed via ^1H NMR and ^{13}C NMR spectroscopy as well as by elemental analysis.

3.2 Synthesis and Characterization of the Copolymers

The reversible crosslinkable terpolymers, bearing both furfuryl and maleimide functionalities with different linkers, were prepared by a copolymerization of different polar and nonpolar methacrylates (RMA), respectively, with furfuryl methacrylate (FMA) and MIMA 1, MIMA 2 or MIMA 3 (**Scheme 2**). The atom transfer radical polymerization (ATRP) procedure was applied using ethyl 2-bromoisobutyrate (EBiB) as initiator, CuBr as catalyst and 1,1,4,7,10,10-hexamethyltriethylene-tetramine (HMTETA) as ligand at a temperature of 70 °C in toluene as solvent or at room temperature in DMF, respectively. The reaction conditions for the terpolymers with the polar co-monomers (**P1**, **P2** and **P4**) were varied due to the better solubility in polar solvents [33,34]. But it was also possible to synthesize a terpolymer with DMEAMA with toluene as solvent at a temperature of 70 °C (**P6**). A co-monomer to functional monomer ratio of 8:1:1 was used, following our previous work as the best ratio to obtain optimal self-healing properties [20]. Selected properties of the polymers with different maleimide methacrylate monomers, polar and nonpolar co-monomers, the reaction conditions and the calculations of the molar masses and molar mass distributions, obtained from SEC measurements, are listed in **Table 1**.

^1H NMR spectroscopy was utilized for the structural characterization of the RMA-*co*-FMA-*co*-MIMA 1, MIMA 2 or MIMA 3 copolymers. **Figure 1** shows the ^1H NMR spectra of **P6** and **P7**, respectively. The signals from the saturated protons ($-\text{CH}_3$ and $-\text{CH}_2$) of the methacrylate backbone are correlated to the signals 0.4 to 2.1 ppm.

Additionally, the signals of the aromatic protons of the furfuryl groups are assignable to the signals 7.4 and 6.4 ppm. The signals corresponding to the protecting furan groups of the maleimide functionalities are visible at 6.6 and 5.3 ppm, respectively. Additionally, further signals at 3.0 ppm could also be assigned to the maleimide group. Moreover, the signal at 3.9 ppm belongs to the methylene groups of the co-monomers. The signals “4”, “6” and “9” have been utilized to determine the composition of the polymers. The different monomer ratios of the copolymers and the theoretical crosslinking densities are summarized in **Table 2**.

3.3 Thermal Properties of the Copolymers

The potential of the self-healing abilities of the copolymers **P1** to **P7** was investigated by DSC measurements. The presence of specific transitions during the heating and cooling cycles represents an important precondition for the suitability of the polymers of self-healing applications. In the first heating curve a large endothermic peak should be visible, assignable to the energy which is required for the retro-Diels-Alder reaction and the subsequent evaporation of the maleimide protecting group (*i.e.* furan). This behavior could be observed by using a simultaneous thermal analysis (STA) of the copolymer **P7*** of the previous work [20], where the mass loss of the furan is visible between 120 to 160 °C and the corresponding MS spectra shows two additional peaks at 39 and 68 m/z at a temperature of 151 °C corresponding to the evaporating furan molecules (**Figure 2**) [35]. The lower mass signals belong to the background measurement.

Moreover, the glass transition temperatures (T_g) of the protected and, therefore, non-crosslinked copolymers should be observed. The T_g of the polymer will also have an influence on the mechanical film properties of the resulting polymer film. In the non-

crosslinked state and, therefore, also during the self-healing process, a lower T_g will result in softer films compared to a high T_g monomer, which is beneficial for the self-healing. However, the crosslinking will lead to harder polymer films. A co-monomer with a low T_g still results in crosslinked films which feature mechanical properties comparable to non-crosslinked PMMA [20,21]. Most significant in the second heating curve is the presence of the endothermic peak of the retro-Diels-Alder reaction, even though the area below the curve will be smaller, because the energy of the evaporation of the furan is missing and only the energy of the retro-Diels-Alder reaction is observable. It was anticipated that the polar surrounding of the functional groups could influence the T_{RDA} . Nevertheless, the appearance of this peak in the second heating curve represents also an important precondition for the self-healing properties of the copolymers. These properties depend on the structural composition of the copolymer, like the co-monomer and the linker of the maleimide. They influence the flexibility/mobility of the chain and the glass transition temperature. The summary of the DSC results of the copolymers is listed in **Table 3**.

The DSC measurements of copolymer **P1** reveal in the first heating curve a usual T_{RDA} between 120 to 180 °C, only in the second heating curve the T_{RDA} already started at 100 °C. The T_g of copolymer **P1** is slightly lower than in HEMA homopolymers due to the flexible furan and the maleimide monomers [36]. For **P2** no change of the T_{RDA} could be observed. Also in case of **P3** and **P4** with MIMA 2 no significant decrease of the T_{RDA} could be detected. Only the T_g of the DMAEMA copolymer is low comparable to the BMA copolymer. This effect should be beneficial for the self-healing abilities of the copolymer. The T_g of DMAEMA homopolymers is around 4 °C and for the BMA homopolymers around 17 °C [37,38]. The same trend is visible for the materials **P5** and **P6** with BMA and DMAEMA and the MIMA 3 with the oxygen-containing linker. Also

in this case the T_{RDA} is not significantly decreased (only 10 °C for the BMA copolymer **P5**). The glass transition temperature is also lower for copolymer **P5** compared to **P3**. This behavior is caused by the oxygen-containing linker of the maleimide. Copolymer **P3** revealed the same glass transition temperature as copolymer **P5***, in spite of the longer linker; only copolymer **P5** with the oxygen-containing linker showed a lower T_g . However, the temperature of the retro-Diels-Alder reaction for copolymers **P3** to **P6** is slightly decreased compared to copolymer **P5***. Copolymer **P7** with the DEGMA as comonomer has the lowest glass transition temperature of -10 °C, but also in that case the T_{RDA} could not be decreased significantly (only 5 °C lower than the usually observed temperature between 120 to 180 °C). An interesting finding is the presence of a glass transition temperature in the second heating curve for copolymers **P5** to **P7**. In the case of copolymer **P5** and **P6** the T_g in the second heating curve is higher due to the crosslinking; but this is not the case for copolymer **P5**. Nevertheless, the glass transition temperatures of the copolymers **P1** to **P6** are not lower as the T_g of **P7***, which revealed the best self-healing properties in the earlier published work [20]; only copolymer **P7** has a comparable glass transition temperature. Also the T_{RDA} of the new copolymers are comparable to the T_{RDA} of copolymer **P7***, only **P3**, **P5** and **P7** showed a slightly decreased T_{RDA} in the second heating curve. The DSC traces for copolymer **P5** are also depicted in **Figure 3**. In the second heating curve there are also two peaks visible for the retro-Diels-Alder reaction, because the retro-Diels-Alder reaction for the endo-product occurs at lower temperatures than for the exo-product, due to the fact that the endo-product is the kinetically and the exo-product the thermodynamically preferred state [39].

In the TGA measurements of the copolymers the mass loss of the maleimide protecting group (furan) is observable. By using ^1H NMR spectroscopy the theoretical mass loss

was estimated from the calculated monomer ratios. In **Table 3** the comparison of the temperature of the evaporation with the theoretical and the measured mass loss are listed. The temperatures of the mass loss are in the expected range between 120 to 180 °C. Only for copolymer **P1** the deprotection occurred at lower temperatures. The theoretical and the calculated mass losses correlate very well, only copolymer **P1** revealed larger differences, which are presumably due to degradation processes, which take place at higher temperatures.

3.4 Self-healing studies of the Copolymers

Due to the used co-monomers resulting in very high T_g and T_{RDA} values no self-healing studies were performed with **P1** and **P2**. The study of the self-healing properties of copolymers **P3** to **P7** was performed by using a microscope with a camera for visualization, because with this setup also real-time self-healing measurements of large scratches could be visualized. Copolymers **P3** and **P5** with the BMA co-monomer and the MIMA 2 and 3 with the longer linker showed good self-healing properties. The surface is not as smooth as obtained in the previously published work with the LMA co-monomer [20], but an acceptable film quality could be obtained. The self-healing studies of copolymer **P3** is depicted in **Figure 4**. The scratch in a millimeter range could be healed completely at 140 °C after 3 min and also at 110 °C after 3 h the scratch was nearly healed. Copolymer **P3** shows improved self-healing properties compared to copolymer **P5***, because in the previous case only scratches in the nanometer range could be healed using higher temperatures of 170 °C after 2 h [20]. The materials have also slightly better self-healing properties compared to copolymer **P7*** (20 °C lower healing temperature). Copolymer **P4** showed no self-healing behavior in the investigated temperature range because the copolymer was too stiff with many defects

of the film due to the furan evaporation after crosslinking and, therefore, no reflow of the damaged parts was possible, despite of the low glass transition temperature.

The self-healing studies of copolymer **P5** is depicted in **Figure 5**. The scratch could be healed completely at 140 °C after 5 min and also at 80 °C after 48 h the scratch was nearly gone. Copolymer **P6** showed also self-healing behavior at temperatures above 120 °C in a timescale of 5 min, but the surface of the coating was not as smooth as the surface of **P5**. Copolymers **P5** and **P6** revealed also better self-healing properties compared to copolymer **P5*** with regard to the size of the healed scratch and the lower healing temperatures, also in comparison to copolymer **P7*** in respect to the lower self-healing temperature.

The self-healing studies of copolymer **P7** is depicted in **Figure 5**. Compared to the previous copolymer **P7** was annealed after deprotection of the maleimide group overnight at 40 °C to improve the crosslinking density and for hardening of the film. The longer hardening times for oxygen-containing system were also observed by Mayo *et al.* [32]. They pointed out that their oxygen-containing linker requires more time for the subsequent crosslinking compared to the alkyl, cyclic as well as aryl linker and also reveals excellent film-forming characteristics. The surface of the copolymer **P7** is also as smooth as obtained by copolymer **P7***. As showed in **Figure 6** the smaller scratch could be healed completely at 100 °C after 2 h and the larger ones after 4 h. Also at lower temperatures of 80 °C the scratch could be healed after 24 h partially. The copolymer **P7** has the best film-forming and self-healing properties of all synthesized polymers. Additionally, **P7** features also a lower healing temperature than copolymer **P7*** due to the higher flexibility of the linker unit in combination with the DEGMA.

4. Conclusion

The synthesis of new terpolymers with MIMA 1, MIMA 2 and MIMA 3 with three different linkers and FMA as functional units for Diels-Alder reactions and different polar and nonpolar co-monomers could be accomplished. As polar co-monomers hydroxyethyl methacrylate (HEMA), dimethylaminoethyl methacrylate (DMAEMA) and 2-(hydroxyethoxy)ethyl methacrylate (DEGMA) and as nonpolar co-monomers butyl methacrylate (BMA) were utilized. The polymers were prepared *via* ATRP with CuBr as catalyst, HMTETA as ligand and EB*i*B as initiator at 70 °C in toluene or at room temperature in DMF. Furthermore, the characterization was carried out using ¹H NMR spectroscopy, SEC, TGA and DSC measurements. The self-healing properties of the copolymers were studied using a microscope with a camera for real-time analyses. Copolymers **P3** and **P5** with BMA and the MIMA 2 and 3 with the longer alkyl chain and the oxygen-containing linker revealed superior self-healing behavior compared to the previously described “all-in-one” system **P7***. These materials were able to completely heal scratches on the millimeter range at 140 °C. Copolymer **P7** with DEGMA and the oxygen-containing linker reveals the best self-healing performance of all synthesized polymers. A low healing temperature of 100 °C could be achieved by the introduction of the linker unit featuring a higher flexibility in combination with DEGMA. In contrast to other examples described, polar co-monomers did not significantly influence the temperature of the retro-Diels-Alder reaction in these polymeric systems. Nevertheless, the required healing temperature could be decreased significantly compared to copolymer **P7***. In summary, an alternative for the one-component self-healing system of the previously published work could be developed with shorter side chains (BMA) and a polar side chain (DEGMA) combined with a longer as well as an oxygen-containing linker for the MIMA. In contrast to the rather

small influence of the nature of the co-monomer (as long as it features a low T_g) the nature of the linker unit revealed a significant influence on the resulting properties enabling an enhancement of the self-healing properties.

Acknowledgements: This study was supported by the Deutsche Forschungsgemeinschaft (SPP 1568).

References

- [1] Goussé C, Gandini A, Hodge P. *Macromolecules* 1998;31(2):314–21.
- [2] Murphy EB, Bolanos E, Schaffner-Hamann C, Wudl F, Nutt SR, Auad ML. *Macromolecules* 2008;41(14):5203–9.
- [3] Peterson AM, Jensen RE, Palmese GR. *ACS Appl. Mater. Interfaces* 2010;2(4):1141–9.
- [4] Bergman SD, Wudl F. *J. Mater. Chem.* 2007;18(1):41–62.
- [5] Hager MD, Greil P, Leyens C, van der Zwaag, Sybrand, Schubert US. *Adv. Mater.* 2010;22(47):5424–30.
- [6] Chujo Y, Sada K, Saegusa T. *Macromolecules* 1990;23(10):2636–41.
- [7] Canary SA, Stevens MP. *J. Polym. Sci., Part A: Polym. Chem.* 1992;30(8):1755–60.
- [8] Laita H, Boufi S, Gandini A. *Eur. Polym. J.* 1997;33(8):1203–11.
- [9] Gheneim R, Perez-Berumen C, Gandini A. *Macromolecules* 2002;35(19):7246–53.
- [10] Gandini A, Coelho D, Silvestre AJ. *Eur. Polym. J.* 2008;44(12):4029–36.
- [11] Chen X, Dam MA, Ono K, Mal AK, Shen H, Nutt SR et al. *Science* 2002;295(5560):1698–702.
- [12] Chen X, Wudl F, Mal AK, Shen H, Nutt SR. *Macromolecules* 2003;36(6):1802–7.

- [13] Se Park J, Takahashi K, Guo Z, Wang Y, Bolanos E, Hamann-Schaffner C et al. J. Compos. Mater. 2008;42(26):2869–81.
- [14] Wouters M, Craenmehr E, Tempelaars K, Fischer H, Stroeks N, van Zanten J. Prog. Org. Coat. 2009;64(2-3):156–62.
- [15] Syrett JA, Mantovani G, Barton, William R. S., Price D, Haddleton DM. Polym. Chem. 2010;1(1):102–6.
- [16] Kavitha AA, Singha NK. J. Polym. Sci., Part A: Polym. Chem. 2007;45(19):4441–9.
- [17] Kavitha AA, Singha NK. Macromol. Chem. Phys. 2007;208(23):2569–77.
- [18] Kavitha AA, Singha NK. ACS Appl. Mater. Interfaces 2009;1(7):1427–36.
- [19] Kavitha AA, Singha NK. Macromolecules 2010;43(7):3193–205.
- [20] Kötteritzsch J, Stumpf S, Hoepfener S, Vitz J, Hager MD, Schubert US. Macromol. Chem. Phys. 2013;214(14):1636–49.
- [21] Bose RK, Kötteritzsch J, Garcia SJ, Hager MD, Schubert US, van der Zwaag, Sybrand. J. Polym. Sci. Part A: Polym. Chem. 2014;52(12):1669–75.
- [22] Barthel MJ, Rudolph T, Crotty S, Schacher FH, Schubert US. J. Polym. Sci., Part A: Polym. Chem. 2012;50(23):4958–65.
- [23] Barthel MJ, Rudolph T, Teichler A, Paulus RM, Vitz J, Hoepfener S et al. Adv. Funct. Mater. 2013;23(39):4921–32.
- [24] Rudolph T, Barthel MJ, Kretschmer F, Mansfeld U, Hoepfener S, Hager MD et al. Macromol. Rapid Commun. 2014;35(9):916–21.
- [25] Du P, Wu M, Liu X, Zheng Z, Wang X, Joncheray T et al. J. Appl. Polym. Sci. 2014;131(9):40234.
- [26] Heo Y, Sodano HA. Adv. Funct. Mater. 2014;24(33):5261–8.

- [27] Ikezaki T, Matsuoka R, Hatanaka K, Yoshie N. *J. Polym. Sci. Part A: Polym. Chem.* 2014;52(2):216–22.
- [28] Toncelli C, De Reus, Dennis C., Picchioni F, Broekhuis AA. *Macromol. Chem. Phys.* 2012;213(2):157–65.
- [29] Wijnen JW, Engberts JBFN. *J. Org. Chem.* 1997;62(7):2039–44.
- [30] Rispens T, Engberts JBFN. *J. Phys. Org. Chem.* 2005;18(8):725–36.
- [31] Kiselev VD, Konovalov AI. *J. Phys. Org. Chem.* 2009;22(5):466–83.
- [32] Mayo JD, Adronov A. *J. Polym. Sci. Part A: Polym. Chem.* 2013;51(23):5056–66.
- [33] He W, Jiang H, Zhang L, Cheng Z, Zhu X. *Polym. Chem.* 2013;4(10):2919–38.
- [34] Guice KB, Loo Y. *Macromolecules* 2006;39(7):2474–80.
- [35] AIST: Integrated Spectral Database System of Organic Compounds. (Data were obtained from the National Institute of Advanced Industrial Science and Technology (Japan)).
- [36] Russell GA, Hiltner PA, Gregonis DE, de Visser AC, Andrade JD. *J. Polym. Sci. Polym. Phys. Ed.* 1980;18(6):1271–83.
- [37] Teoh RL, Guice KB, Loo Y. *Macromolecules* 2006;39(25):8609–15.
- [38] Liu G, Zhang L, Wang Y, Zhao P. *J. Appl. Polym. Sci.* 2009;114(6):3939–44.
- [39] Canadell J, Fischer H, With G de, van Benthem RATM. *J. Polym. Sci., Part A: Polym. Chem.* 2010;48(15):3456–67.

Scheme and Figure Captions:

Scheme 1: Schematic representation of the synthesis of the maleimide methacrylate monomers (MIMA 1, MIMA 2 and MIMA 3).

Scheme 2: Schematic representation of the copolymerization of different polar and nonpolar methacrylates (RMA), FMA and MIMA 1, MIMA 2 and MIMA 3 by ATRP.

Figure 1: ^1H NMR spectra of **P6** (left) and **P7** (right) (in CDCl_3).

Figure 2: STA measurement of copolymer **P7***: TGA (left), MS spectra at 29 and 151 $^\circ\text{C}$ (right).

Figure 3: DSC analysis of copolymer **P5**.

Figure 4: Self-healing experiment of copolymer **P3** using a microscope for visualization. a) to c) Healing experiments at 140 $^\circ\text{C}$, a) scratch before annealing, b) scratch after annealing for 1 min and c) scratch after annealing for 3 min and d) to f) healing experiments at 110 $^\circ\text{C}$, d) scratch before annealing, e) scratch after annealing for 30 min and f) scratch after annealing for 3 h.

Figure 5: Self-healing experiment of copolymer **P5** using a microscope for visualization. a) to c) Healing experiments at 140 $^\circ\text{C}$, a) scratch before annealing, b) scratch after annealing for 2 min and c) scratch after annealing for 5 min and d) to f) healing experiments at 80 $^\circ\text{C}$, d) scratch before annealing, e) scratch after annealing for 2 h and f) scratch after annealing for 48 h.

Figure 6: Self-healing experiment of copolymer **P7** using a microscope for visualization. a) to d) Healing experiments at 100 $^\circ\text{C}$, a) scratch before annealing, b) scratch after annealing for 1 h, c) scratch after annealing for 2 h, d) scratch after annealing for 4 h and e) to f) healing experiments at 80 $^\circ\text{C}$, e) scratch before annealing,

f) scratch after annealing for 24 h. Pretreatment: Annealing at 130 °C for 3 h and at 40 °C overnight.

ACCEPTED MANUSCRIPT

Tables:

Table 1: Comparison of the different maleimide methacrylates, the co-monomers and the reaction conditions of the copolymers, the theoretical molar mass and the molar mass and molar mass distributions of the copolymers measured by SEC.

Polymer	MIMA	Co-monomer	Reaction conditions	M_n (theo) [g/mol]	M_n(SEC)^{a)} [g/mol]	PDI (SEC)
P1	MIMA 1	HEMA	DMF, r. t.	3,710	12,090	1.48
P2	MIMA 1	DMAEMA	DMF, r. t.	8,510	9,860	1.69
P3	MIMA 2	BMA	toluene, 70 °C	8,190	4,910	1.33
P4	MIMA 2	DMAEMA	DMF, r. t.	8,790	7,490	1.69
P5	MIMA 3	BMA	toluene, 70 °C	4,060	4,330	1.36
P6	MIMA 3	DMAEMA	toluene, 70 °C	4,360	4,440	1.33
P7	MIMA 3	DEGMA	toluene, 70 °C	4,980	3,100	1.41

^{a)} (SEC conditions: DMAc with 2.1 g/L LiCl as solvent, PMMA as standard for the calibration)

Table 2: Comparison of the theoretical and calculated ratios of the co-monomers and the theoretical crosslinking density.

Polymer	Ratio of the co-monomers	Theoretical^{a)}	Calculated^{a)}	Crosslinking density_{theo}^{b)} [%]
P1	HEMA:FMA	8:1	7:1	23
	HEMA:MIMA 1	8:1	5:1	
P2	DMAEMA:FMA	8:1	6:1	26
	DMAEMA:MIMA 1	8:1	7:1	
P3	BMA:FMA	8:1	6:1	30
	BMA:MIMA 2	8:1	7:1	
P4	DMAEMA:FMA	8:1	5:1	15
	DMAEMA:MIMA 2	8:1	11:1	
P5	BMA:FMA	8:1	8:1	25
	BMA:MIMA 3	8:1	9:1	
P6	DMAEMA:FMA	8:1	7:1	22
	DMAEMA:MIMA 3	8:1	9:1	
P7	DEGMA:FMA	8:1	6:1	11
	DEGMA:MIMA 3	8:1	14:1	

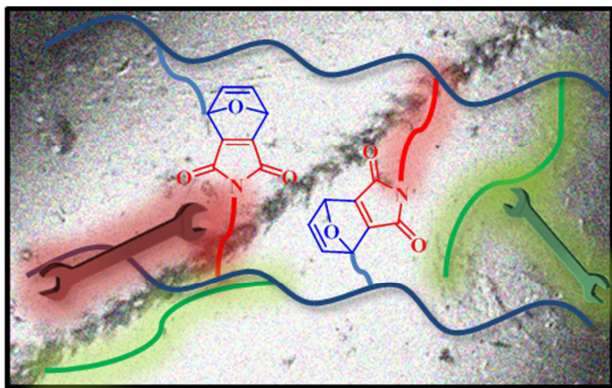
^{a)} The theoretical and calculated molar ratios.

^{b)} The crosslinking density is calculated by weight.

Table 3: Comparison of the glass transition temperatures (T_g) and the temperature of the retro-Diels-Alder reaction (T_{RDA}) of the copolymers measured by DSC as well as the temperature of evaporation of the protecting group (T_{evap}) and the theoretical as well as the calculated ratios of the co-monomers obtained by TGA.

Polymer	DSC measurements			TGA measurements		
	Heating curve	T_g [°C]	T_{RDA} [°C]	T_{evap} [°C]	mass loss _{theo} [%]	mass loss _{exp} [%]
P1	1 st	80	120 to 180	100 to 180	5	19
	2 nd	-	100 to 180			
P2	1 st	50	125 to 170	130 to 160	7	6
	2 nd	-	120 to 170			
P3	1 st	50	125 to 180	120 to 180	5	6
	2 nd	-	115 to 180			
P4	1 st	25	125 to 180	120 to 160	5	4
	2 nd	-	120 to 180			
P5	1 st	40	120 to 180	135 to 170	4	4
	2 nd	60	110 to 180			
P6	1 st	35	120 to 180	130 to 180	4	4
	2 nd	40	120 to 180			
P7	1 st	-10	120 to 180	125 to 175	4	3
	2 nd	-10	115 to 160			
P5*^{a)}	1 st	50	140 to 180	140 to 180	5	6
	2 nd	-	140 to 180			
P7*^{a)}	1 st	-16	120 to 180	132 to 163	4	4
	2 nd	-	120 to 190			

^{a)} Polymers of the previous publication [20]; **P5*** represents P(BMA-*co*-FMA-*co*-MIMA 1) and **P7*** represents P(LMA-*co*-FMA-*co*-MIMA 1) with 20 mol-% functionality.



ACCEPTED MANUSCRIPT

